Journal of Sciences, Islamic Republic of Iran 22(1): 33-49 (2011) http://jsciences.ut.ac.ir
University of Tehran, ISSN 1016-1104

Signatures of the Balarud Deep Seated Fault Zone in Khushab Anticline, SW Iran, An Integrated Study

H. Hajialibeigi,[1,*] S.A. Alavi,[1] J. Eftekharnezhad,[2]
M. Mokhtari,[3] and M.H. Adabi[1]

[1]*Department of Geology, Faculty of Science, Shahid Beheshti University, Tehran, Islamic Republic of Iran*
[2]*Geological Survey and Mining Exploration of Iran, Tehran, Islamic Republic of Iran*
[3]*International Institute of Earthquake and Seismology, Tehran, Islamic Republic of Iran*

Received: 16 March 2010 / Revised: 26 September 2010 / Accepted: 28 February 2011

Abstract

The Khushab anticline is located in the Zagros fold-thrust belt in the Lurestan. This anticline is affected by the Balarud fault zone, which is a part of Mountain Front Fault between the Lurestan and Dezful Embayment zones. Based on the measurement of the elements of fold style, this anticline is analyzed. According to these measurements, this anticline is a noncylindrical, asymmetrical and disharmonic fold. The anticline is a z-fold and verges slightly to the southwest. The tightness and bluntness of folding suggests that fold is gentle to close and subangular respectively. Broad to wide is suggested as disccriptive term of the aspect ratio. Based on Ramsay's classification the fold is subclass 1B to 1C. The field observations, seismic profiles, cross-sections, analyses of the geometric parameters and comparison of the anticline with the fault-related fold models suggest the anticline as a detachment fold that is probably sheared by this zone. The sinistral shear of this zone, due to a system of shear fractures is discussed. These fractures (C, D, E, F, and G sets) which occur obliquely with respect to fold axis are shear fractures. Another fracture system including A and B sets are parallel and perpendicular to fold axis respectively. These fractures formed in association with folding. It seems that two phases are responsible for forming of these fractures. A and B sets were formed in first phase and associated with formation of anticline. The shear fracture system was formed in second phase and is under effect of this zone.

Keywords: Balarud fault zone; Khushab anticline; Detachment folding; Zagros fold-thrust belt

Introduction

The structural geologists, who have worked in fold-thrust belts, have recognized relationships between folds and thrusts (e.g. [12,13,17,23,18,73,37,50,56,80,20,83]). Based on these relationships and field observation or seismic profiles, they have categorized the folded structures in these belts, and have defined different fold types.

* Corresponding author, Tel.: +98(21)29902600, Fax: +98(21)29902628, E-mail: h-alibeigi@cc.sbu.ac.ir

Detachment (or decollement) folds are one of these folded structures have been discussed by [40,37,49,18,38,29,34,60,51. These folds form by displacement and differential shortening of the hangingwall above a bedding-parallel fault, or detachment horizon [18], which may occur either at a fault tip or within a thrust sheet [29,37,49] or faulted detachment folds [51]. In this type of folding, differential shortening is independent of the propagation in decollement, which can be accommodated above a fault [39]. Due to the wide range of possible detachment fold geometries, no simple geometric or kinematics model for detachment folding exists [34]. These folds are generally more symmetric than other fold form in fold-thrust belts [52].

The concentric folds of the Zagros fold-thrust belt have been interpreted as detachment folds by [1,2,16]. Also [45] have suggested that many of the folds within the Zagros fold-thrust belt (especially in Lurestan zone) are detachment folds. The different aspects of detachment folding in Zagros fold-thrust belt have discussed by [69]. They have presented different arguments showing that the most of folds in this fold-thrust belt are in agreement with models of detachment folding proposed by former authors: [18,59,52].

The main propose of this paper is the indication of the geometric effects of the Balarud deep seated fault zone [61], and the mechanism folding of the Khushab anticline. Due to approach this proposes, based on the field observations and seismic profiles the geometry of the Khushab anticline (Fig. 1) has been discussed. Several sets of fold-related and fault-related fractures, which collected during field observations has been analyzed. These fractures, which were constituted the two systems, one including two fractures sets (A and B sets) are orthogonal. And the second fracture system, including five fractures sets (C, D, E, F, and G sets) are oblique with respect to anticline axis. Further, the effects of the Balarud fault zone, or the mechanism(s) responsible for formation of the Khushab anticline has been evaluated. Finally, it has been determined that Khushab anticline is a detachment fold.

Geological Background and Tectonics Setting

Outcrop of the Khushab anticline, is about 30 Km long and up to 12 Km wide and lies in Zagros fold-thrust belt, about 80 Km Northeast of Andimeshk. The anticline has NW-SE trend and locating between Rit (in Northeast) and Chenareh (in Southwest) anticlines (Figs. 1, 2 & 3). These structures are affected by the Balarud fault zone [59]. This zone has sinistral movement [61], is a part of the Mountain Front Fault in Zagros fold-thrust belt [21,22,11] (Fig. 1). Due to the movement of this zone, the ends of major Lurestan anticlines have been deflected [61].

The E-W trending Balarud fault zone is the boundary between the Lurestan (in North) and the Dezful Embayment zone (in South) (Fig. 1). This fault zone is a basement-involved and active fault zone [11], and is considered as oblique lateral ramp that is responsible for

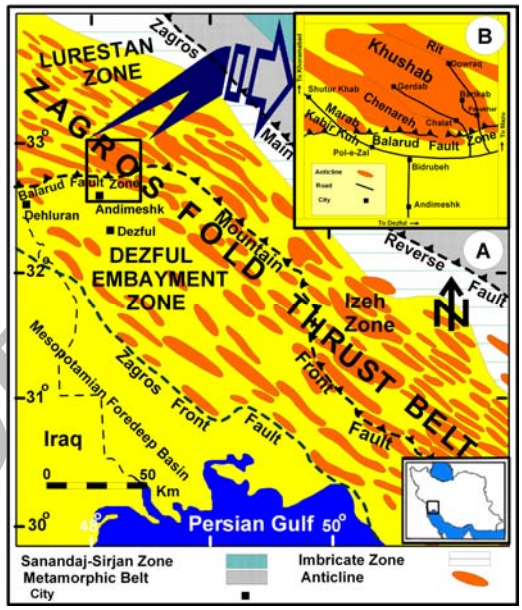

Figure 1. Simplified map of the western Zagros orogenic system (Modified after [58]). Inset map of Khushab anticline and adjacent anticlines that are affected by the Balarud blind thrust fault zone.

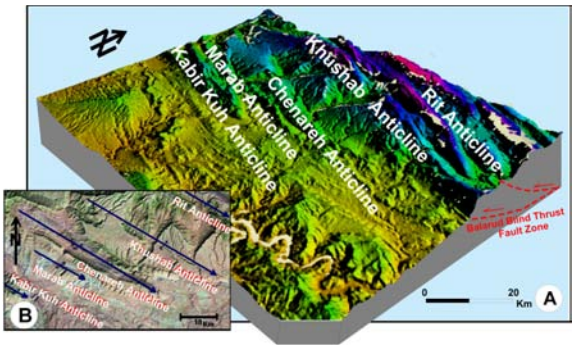

Figure 2. DEM (Digital Elevation Modeling) of Khushab anticline and other adjacent anticlines it. Inset Landsat TM image of Rit, Khushab, Chenareh, Marab, Kabir Kuh anticlines.

Table 1. Simplified stratigraphic column of the area between the Lurestan and Dezful Embayment zones (modified from [54,3,39,72,22,16,48,59]). Positions of the main detachment horizons in the Khushab anticline are marked with arrow

System/Series	Symbols	Thick (m)	Stratigraphy
Plio-Pliostocene	Q_2	-	Alluvium
	Q_1	-	Recent Conglomerate
Miocene	L_{bm}	500-3000	Lahbari Member (Limestone and Sandstone)
	A_j		Agha Jari Formation [Sanstone and Silstone]
	G_s	200-750	Gachsaran Formation[Gypsum,Salt and Silstone] (←)
Oligocene	A_s	200-450	Asmari-Shahbazan Formation [Limestone and Dolomite]
Palocene-Eocene	K_n	250-900	Kashkan Formation [Fleysh Clastic,Siltstone Sanstone and Conglomerate,]
	T_z		
	A_m		Taleh Zang Formation [Limestone]
	P_b		Amiran Formation [Siltstone and Sandstone] (←) Pabdeh Formation [Marl Limestone,Shale and Marl](←)
Cretaceous	G_u	150-500	Gurpi Formation [Carbonate Shales] (←)
	B_{gp}	900-1200	Bangestan Group [Thick and Thin bedded Limestone and shale]
	G_u	900	Garau Formation [Limstone Shale] (←)
Triassic- Jurassic	K_{gp} & N_z	-	Kazerun Group &Neyriz Formation[Shale, Marl,Dolomite and Evaporate Deposits]
	D_k	40-900	Dashtak Formation [Shale,Dolomite and Evaporate] (←)
Permian	D_{gp}	-	Deh ram Group [Dhale,Marl, Limestone Dolomite, Sandstone and Evaporate Deposits]

the variation in facieses and thickness [68], on both sides of the fault zone. Based on field observations, satellite image and geological maps the trend of the Balarud fault zone can be characterized as En echelon series of anticlines [61]. Among these structures, the Khushab anticline associated with adjacent anticlines (due to their trends [61]) which mainly affected by above mentioned fault zone (Figs. 1 & 2).

Tectonosedimentary evolution of the Khushab anticline is similar to the Lurestan zone which has been affected by the Balarud fault zone [61].

The stratigraphic column of the area between the Lurestan and Dezful Embayment zones from Deh Ram Group through recent strata is represented in Table 1. A main part of this table mainly consists of the competent units. Also there are several incompetents units, e.g. Pabdeh Formation, Gurpi Formation, Amiran Formation, Dashtak Formation (evaporate depositions) and Garau Formation (limestone shale). These incompetent units are considered as detachment horizons [59,62,16,48]. These horizons play important roles for the structural style of the Khushab and other adjacent anticlines in the region.

Materials and Methods

The following interpretation of the structural evolution of the Balarud fault zone is based on detailed knowledge of the correlation of deformation between basement and overburden units in the Khushab anticline.

Detailed field work (especially on fractures) and geometrical analysis enabled us to distinguish the different deformational effects in the subsurface to determine the different behavior of the Balarud fault zone on overburden units during these deformational

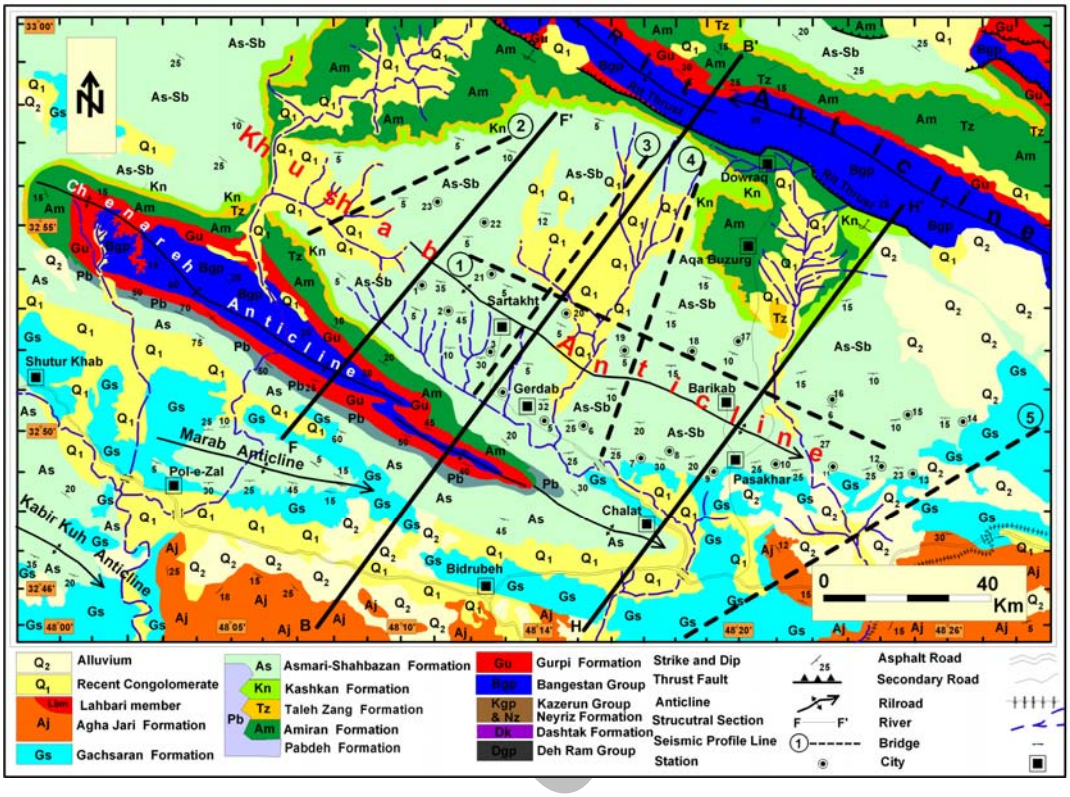

Figure 3. Geological map of Khushab anticline and adjacent anticlines (modified after [43]). Thick straight lines show positions of structural cross-sections that are used in this study. The thick straight line labeled BB' shows position of cross-section of Fig. 12. Dashed lined show position of the seismic profiles.

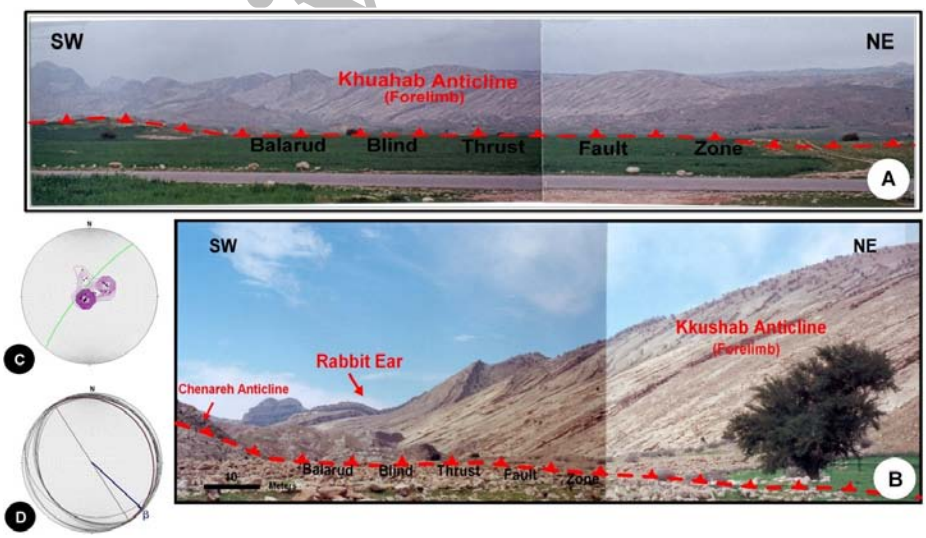

Figure 4. The views of the Khushab anticline and the stereographic projections of it (After [27]). A: The forelimb of Khushab anticline in station No. 9. See location on Fig. 3. B: The forelimb of Khushab anticline and its Rabbit Ear structure in station No. 7. This structure shows involvement of the younger stratigraphic horizons as a minor detachment level. See location on Fig. 3. C and D: Stereographic projection of the Pi (π) and Beta (β) diagrams showing construction of the axis and axial plane for Khushab anticline.

events. Finally, by comparing this anticline with alternative models of the anticline evolution and the theoretical fault-related folding, the mechanism(s) responsible for causing on the Khushab anticline has been evaluated and has been determined the type of the fault-related fold.

The stereographic projection, interpreted seismic profiles, cross-sections and field observations are the databases of this research. In the following sections we describe them:

Stereographic Projection

The strike of the hinge surface of the Khushab anticline is measured from geological map (Fig. 3) to be N55°W. Therefore, the attitude of anticline axis and the axial plane is measured for this anticline 05°/133° and N33°W, 15°NE respectively. In the southwest flank of this anticline (the forelimb) dips of the beddings varies between 5° and 25°. The northeast flank (backlimb) is relatively gently dipping (up to maximum 8°). Khushab anticline plunges 5° toward SE (Figs. 4-B, C, D).

Interpreted Seismic Profiles

Interpretation of the Khushab anticline and adjacent anticlines is constrained by five, 2D time-migrated seismic profiles. The observations on the two lines 3, 4 (Figs. 7, 8) of Khushab structure can be considered as early steps in the development of the fold. A more deformed stage can be observed on two lines 2, 5 (Figs. 6, 9) crossing the Khushab anticline situated further northwest, and further southeast respectively. The interpretation of the seismic profiles 1, 3, 4 through the Khushab anticline suggests the gently backlimb, a slightly shallower dip at the crest, an indistinct forelimb, and a detachment horizon (probably Dashtak Formation ?) (Figs. 5, 7, 8).

The seismic profiles 2, 5 through the Khushab and Chenareh anticlines suggest a shortening on these profiles and the ramp structures in both profiles that the fault exhibits them. Also the interpretation of these seismic profiles suggests that the fault displacement decrease to southwest and dies out in Gachsaran Formation. The simplicity of the Balarud fault zone is better defined in line profile 2 compared with line 5. Based on these lines the geological cross-sections has been constructed (FF', HH', Figs. 10, 11).

Cross-Sections

[43] constructed a cross-section through the Rit, Khushab and Chenareh anticlines (Fig. 12). In their interpretation, they constructed the regional cross-section for this area has been assumed to be near-perfect

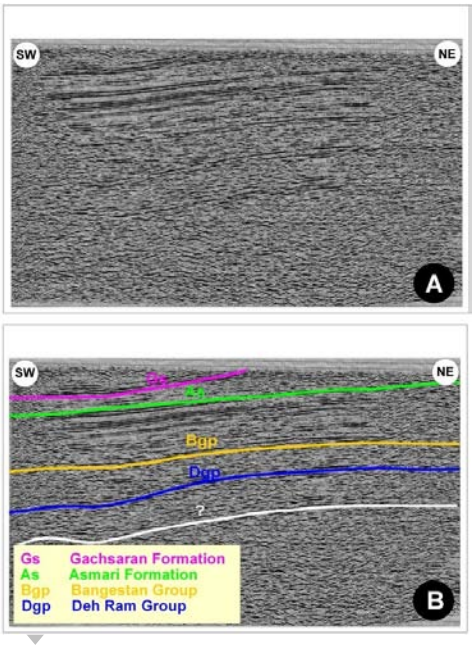

Figure 5. Line 1: Non-interpreted (A) and interpreted (B) versions of seismic profiles cutting as approximately parallel to Khushab anticline axis (After [27]). See location on Fig. 3. This interpreted seismic line across the Khushab anticline, demonstrating the segmentation problem of the Balarud fault zone. See text for more explanation.

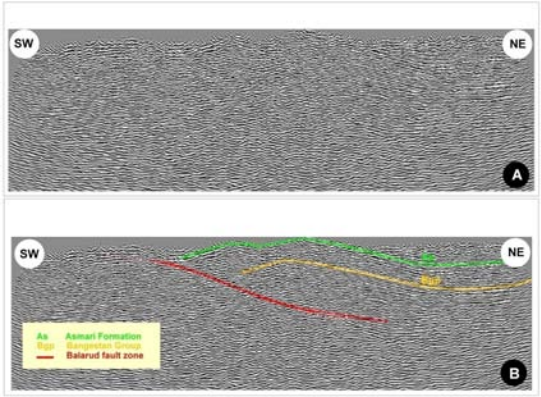

Figure 6. Line 2: Non-interpreted (A) and interpreted (B) versions of seismic profiles cutting as approximately perpendicular to Khushab anticline axis (After [27]). See location on Fig.3. This interpreted seismic line across the Khushab anticline, indicate the Balarud fault zone. See text for more explanation.

concentric folds, without the inclusion of subsurface structures. So, their interpretation was based on surface and filed observations data, and did not consider the 3-D geometries of the structures.

The present study offers an alternative interpretation for the structures in the area, based on consideration of the following factors: (1) the Balarud fault zone behavior based on interpreted seismic profiles (Figs. 5, 6, 7, 8, 9) and surface data (maps and field observations), (2) the locations of the detachment horizons based on the mechanical stratigraphy, and known stratigraphic positions of minor and main detachments in adjacent areas, (3) the projection of surface structures to depth in a series of interpretive cross-sections, using structural styles which are compatible with the mechanical stratigraphy, (4) the use of structural balancing and restoration to test the admissibility and to selection of alternate solutions.

Based on the above factors were integrated to constructed two cross-sections (HH', FF', Figs. 10, 11). These cross-sections, with 22 Km length nearly run perpendicular to the general strike of the bed or folds axes (approximately N40°E trending). Both of the cross-sections were pined at local pin lines in the syncline to southwest of the Khushab anticline and were restored to their undeformed state (Figs. 10, 11). These cross-sections are used in order to study the lateral variations in structural geometry and predication of structural geometry of deep levels and the shortening taken place. On HH' and FF' cross-sections, the fault exhibits a ramp geometry in the middle part of both sections and there is no basement fault in northeast (Figs. 10, 11). This geometry resulted in a fold in hanging wall of ramp in

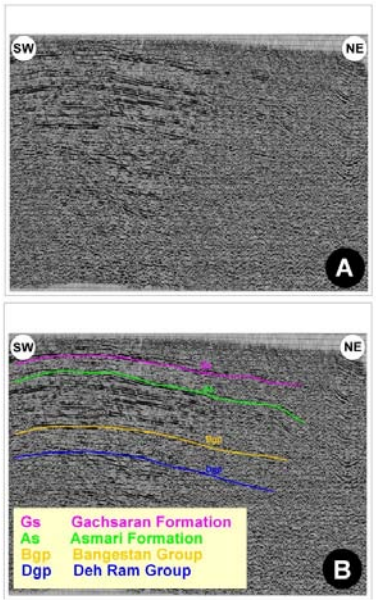

Figure 7. Line 3. Non-interpreted (A) and interpreted (B) versions of seismic profiles cutting as approximately perpendicular to Khushab anticline axis (After [27]). See location on Fig.3. This interpreted seismic line across the Khushab anticline, demonstrating a gap of the segmentation of the Balarud fault zone. See text for more explanation.

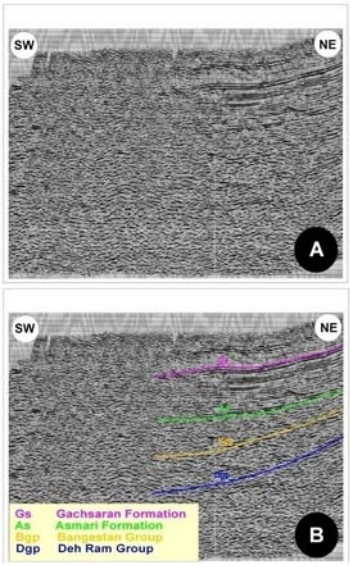

Figure 8. Line 4. Non-interpreted (A) and interpreted (B) versions of seismic profiles cutting as approximately perpendicular to Khushab anticline axis (After [27]). See location on Fig.3. This interpreted seismic line across the Khushab anticline, demonstrating the segmentation problem of the Balarud fault zone. See text for more explanation.

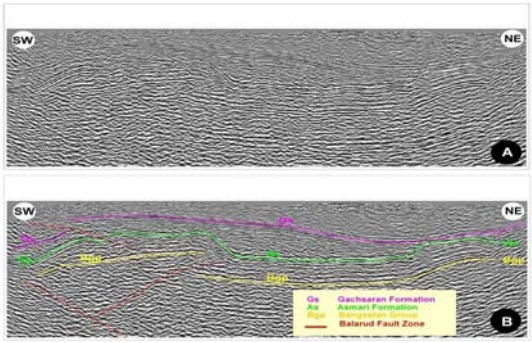

Figure 9. Line 5: Non-interpreted (A) and interpreted (B) the seismic profiles cutting as approximately perpendicular to the Khushab anticline axis (After [27]). See location on Fig.3. This interpreted seismic line across the Khushab anticline, indicate the Balarud fault zone. See text for more explanation.

southwest (Chenareh anticline) and one in northeast (Khushab anticline).

The forelimb dips of Chenareh anticline are slightly greater than those on the backlimb, defining a weak asymmetry with two branches of the Balarud fault zone in HH' cross-section. Also the shortening of the Chenareh anticline is relatively more than the Khushab anticline in both the cross-sections (Figs. 10, 11).

Based on the measurement of different elements of fold [81] and geometric analysis (Fig. 13; Table 2), that is done on these cross-sections [27], it can be stated the anticline is noncylindrical fold. Because of the fold in cross-sections have no mirror plane of symmetry, and the limbs are of unequal length, therefore anticline is called asymmetric fold. In the cross-sections fold dies out within a couple of half-wave lengths or less, so, anticline is disharmonic fold. The anticline is Z-fold, because the short limb has rotated clockwise with respect to the long limbs and the short limb with its two adjacent long limbs. The anticline vergence is slightly toward the southwest. The aspect ratio of fold in FF' and HH' cross-sections are defined as wide and broad respectively. The interlimb angle (í) of the fold decreasing from 129° (in FF' section) to 70° (in HH' section) toward southeast. The tightness of folding, based on the interlimb (í) and folding (φ) angles suggests that fold in FF' and HH' cross-sections is gentle and close respectively. The bluntness is also measured in FF' and HH' cross-sections. Based on this, the relative curvature of the fold at its closure, which is defined by $r_c \leq r_o$ and $0.1 \leq b < 0.2$, is subangular. For the determination of the class of the anticline based on the Ramsay's classification [65] of the folded layers, the calculations and drawings are done on Asmari Formation (Fig. 13). Since, in FF' cross-section, the convergence of dip isogons are toward the inner side of the fold, the curvature of the inner surface is greater than that of the outer surface, and t_α is constant from hinge to limb in all around the fold, therefore this anticline is characterized as subclass 1B. But based on HH' cross-section this anticline is characterized as subclass 1C folds (Table 2).

Field Observations

In the field, several structural elements are observed and have been recorded [27]. These elements are: fractures, stylolites, Rabbit Ear, boudins structures (Figs. 4, 14, 15).

Fractures are collected from 23 stations in the well extension exposure Asmari Formation (Fig. 3). The fractures collected based on procedure that is represented by [19]. Fracture orientation, length, spacing, and mode of deformation (opening or shearing) were recorded as their relationships, evidence for

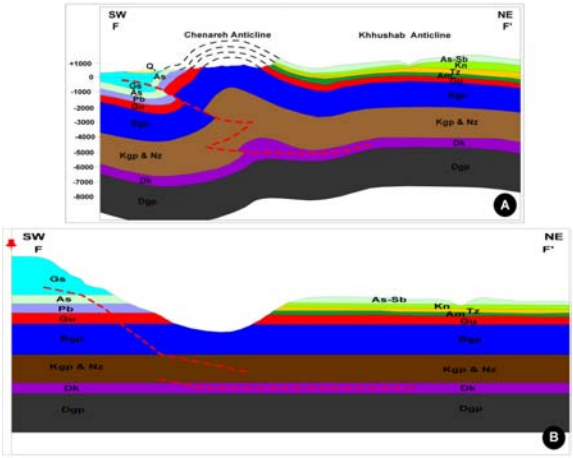

Figure 10. Interpreted structural cross-sections from seismic profiles, surface data (maps and field observation) (After [27]). See location on Fig. 3. Abbreivation: Dehram Group (Dgp), Kazerun Group (Kgp), Neyriz Formation (Nz), Dashtak Formation (Dk), Bangestan Group (Bgp), Kashkan Formation (Kn), Asmari Formation (As), Amiran Formation (Am), Talezang Formation (Tz), Asmari-Shahbazan Formations (As-Sb), Gachsaran Formation (Gs), Recent Conglomerate (Q_1).

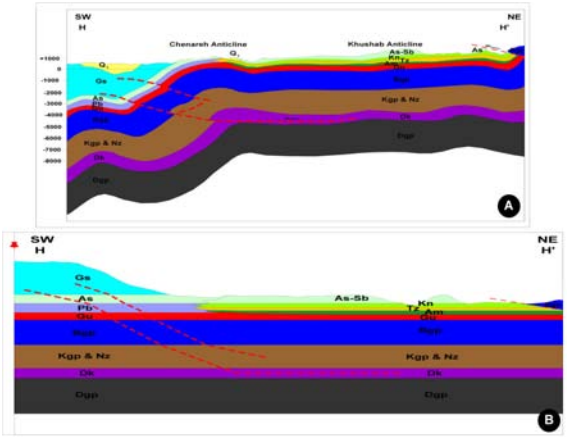

Figure 11. Interpreted structural cross-sections from seismic profiles, surface data (maps and field observation) (After [27]). See location on Fig. 3. Abbreviations: Dehram Group (Dgp), Kazerun Group (Kgp), Neyriz Formation (Nz), Dashtak Formation (Dk), Bangestan Group (Bgp), Kashkan Formation (Kn), Asmari Formation (As), Amiran Formation (Am), Talezang Formation (Tz), Asmari-Shahbazan Formations (As-Sb), Gachsaran Formation (Gs), Recent Conglomerate (Q_1).

fracture reactivation and evidence for fracture infilling. Spacing measurements are parallel to the bedding and are not normalized to bed thickness. The Khushab anticline fractures can be divided in to systematic and nonsystematic.

The nonsystematic fractures, which are locally developed in the anticline but in forelimb with respect to backlimb these fractures, are very well developed. In this research these fractures have taken not into account. The systematic fractures as the fractures pattern are interpreted to identify seven main fractures sets (from A to G sets) (Fig. 14). Two fractures sets (A and B sets) are orthogonal (Figs. 14-A, D). The first (A set) fractures are parallel and father one (B set) perpendicular to anticline axis.

Another fractures sets (C, D, E, F, G sets) (Figs. 14-C, E, F, R) are oblique with respect to anticline axis. A and B sets of fractures are consist of two orthogonal fractures with NW-SE trending and parallel to anticline axis (A set) and others with NE-SW trending and perpendicular to anticline axis (B set). These fractures have developed in all stations expect for stations 3, 4, 9 (in forelimb) and 19, 24 (in backlimb). Only one of two sets (A or B sets) has been observed in these stations. So that fractures with NW-SE trending (parallel to anticline axis) have developed in stations No. 19 and 24 and with NE-SW trending (perpendicular to anticline axis) have developed in stations No. 3 and 9.

In nose zone only one of these sets (A or B sets) has developed, with the exception of stations No. 13 and 10. A and B sets are longer than other sets. Their lengths are 16 and 20 meters respectively. The fractures traces are linear and their spacing varies from 75 centimeters to 2 meters. The oblique fractures sets are: set C (with 090° average strike); set D (with 075° average strike); set E (with 015° average strike); set F (with 345° average strike); set G (with 285° average strike). These fractures sets have mainly developed in forelimb and nose with exception of station No. 16. Set C fractures are linear and with 20 meters long and their spacing varies from 50 centimeters to 2 meters. These fractures are the longest fractures of the oblique set. Set D fractures are 4.5 meters long. Their spacing is similar to set C. set F and E fractures are not very long and are 2-4.5 meters. The spacing of these sets varies from 50 centimeters to 2 meters. Set F and E fractures are less frequency with respect to another set of oblique fractures.

In adition to the above mentioned fractures, several structures have been studied during the field study. In the forelimb, sigmoidal gash fractures (Figs. 14-I, J) and stylolites (Figs. 14-G, H) structures are observed in the Asmari Formation. A Rabbit Ear structure (Fig. 4-B) as a minor anticline, is observed in the forelimb of anticline, in Southwest of the Barikab village (Fig. 3). Also in the forelimb, several boudins structures (Figs.

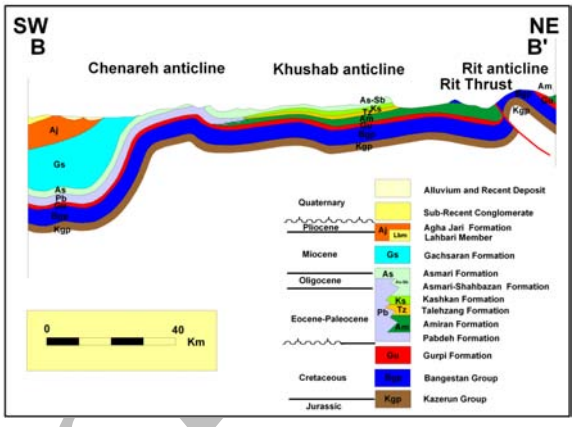

Figure 12. A part of the cross-section BB' across the Rit, Khushab, Chenareh anticlines (After [43]). See location on Fig. 3. Note the cross-section is based on the principle of the concentric folds without attention to the subsurface behavior of the Balarud fault zone. See text for more explanation.

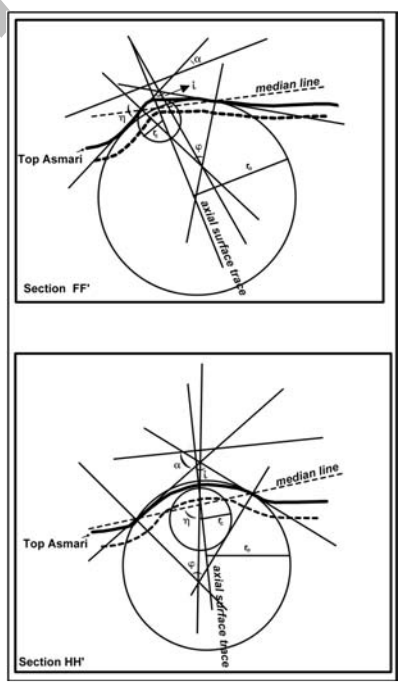

Figure 13. The diagrams have been constructed for to Asmari Formation based on FF' cross-section (A) and HH' cross-section (B) as the style of a folded surface (After [27]). Figures are not to scale. See text for more explanation. Abbreviations: α: dip isogone, í: interlimb angle, φ: folding angle, r_o: reference radius, r_c: closure radius.

Table 2. Geometric analysis for Khushab anticline based on the different parameters (After [27]). See text for more explanation

Section HH'	Section FF'	Cross-sections / Geometrical Characteristics	
70	129	**Interlimb Angle (i)(Degree)**	
110	51	**Folding Angle (φ)(Degree)**	
Noncylindrical Fold	Noncylindrical Fold	**Cylindricity**	
Asymmetrical Fold	Asymmetrical Fold	**Symmetry**	
100	120	**Inclination Angle (η)**	
Z-fold	Z-fold	**Z-fold or S-fold**	
SW	SW	**Vergence**	
Close	Gentle	**Tightness (T)**	
Disharmonic fold	Disharmonic fold	**Harmony**	
0.46	1.169	**P=A/M**	**Aspect Ratio**
0.33	-0.77	**$L_{og}P$**	
Broad	Wide	**Descriptive Term**	
0.6	1.3	**r_c**	**Bluntness**
1.8	5.7	**r_o**	
0.33	0.23	**$r_c/r_o = b$**	
Subangular	Subangular	**Descriptive Term**	
35	24	**α**	**Ramsay's Classification**
0.7	0.7	**T_α**	
0.6	0.6	**T_o**	
0.5	0.65	**t_α**	
0.6	0.6	**t_o**	
1	1.16	**$T'_\alpha = T_\alpha / T_o$**	
0.83	0.6	**$t'_\alpha = t_\alpha / t_o$**	
$t_\alpha < t_o$	$t_\alpha > t_o$	**t_α , t_o**	
$T'_\alpha < S_{ec\,\alpha}$	$T'_\alpha < S_{ec\,\alpha}$	**T'_α , $S_{ec\,\alpha}$**	
$t'_{\alpha<} 1$	$t'_{\alpha=} 1$	**t'_α**	
1C	1B	**Class**	

14-K, L, M), in the margin of river are observed in the Gurpi Formation, and the Gerdab syncline (Fig. 15), in the Southeast of the Gerdab village (Fig. 3) is observed.

Results and Discussion

The structures formed during deformation process reflect control exerted by the reactivation of fault in the underlying basement [24]. Somewhat analogous basement-fault control on the generation of structures in the overlying cover previously has been described [31,32,33,15,79,24,7,57,84,70,8,9,71]. We believe that the Khushab anticline is affected by renewed activity of basement along of the Balarud fault zone.

We analyzed the fractures in this anticline [27]. According to our analyses, A and B sets are orthogonal fractures that have a geometrical relation to the fold elements (e.g. fold axis). These fractures are distinguished including NW-SE trending fractures that are parallel to the fold axis (set A) and the NE-SW trending fractures that are perpendicular to fold axis (set B). Set A fractures are cross fractures type and are open with or without mineral fillings. Set B fractures are longitudinal fracture type and have commonly no

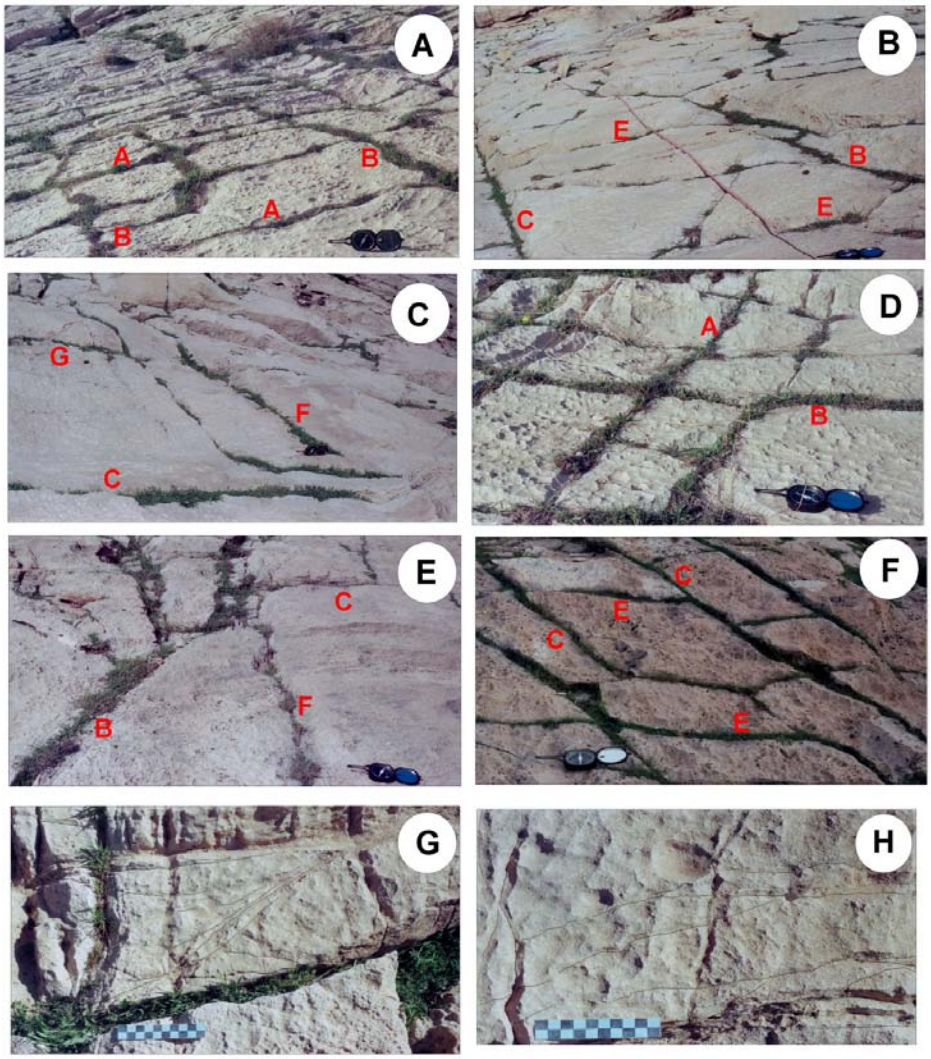

Figure 14. Interpreted field photographs (After [27]). See location on Fig. 3. A: A and B fractures set in Asmari Formation in forelimb of Khushab anticline. Station No. 1. B: Relationship between B, C and E fractures set in Asmari Formation in forelimb of Khushab anticline. Station No. 8. C: F, C and G fractures set in Asmari Formation in forelimb of Khushab anticline. Station No. 12. D: A and B fractures set in Asmari Formation in backlimb of Khushab anticline. Station No. 15. A: Relationship between B, C and F fractures set in Asmari Formation in backlimb of Khushab anticline. Station No. 16. F: C and F fractures set in Asmari Formation in forelimb of Khushab anticline. Station No. 8. G, H: Two examples of observed stylolites in Asmari Formation in forelimb of Khushab anticline. Stations No. 1 and 5.

opening. [82] during the study of the Bangestan anticline fractures have reported parallel and perpendicular fractures to anticline axis. They have considered that these fractures formed during the folding process.

C, D, E, F, G sets are oblique fractures with respect to anticline axis. These fractures which have a geometrical and systematic angular relation to the fault zone, may be interpreted as R', R, P, D shear fractures. These fractures sets confirm with Tchalenco's model in the sinisteral shear zones [78]. According to this model, E-W trending fractures (set C) are D shear fractures. Set C fractures are more abundant with respect to other sets that are oblique fractures. Set C fractures are more developed in forelimb and backlimb with respect to nose. [47] discussed these fractures during the study of

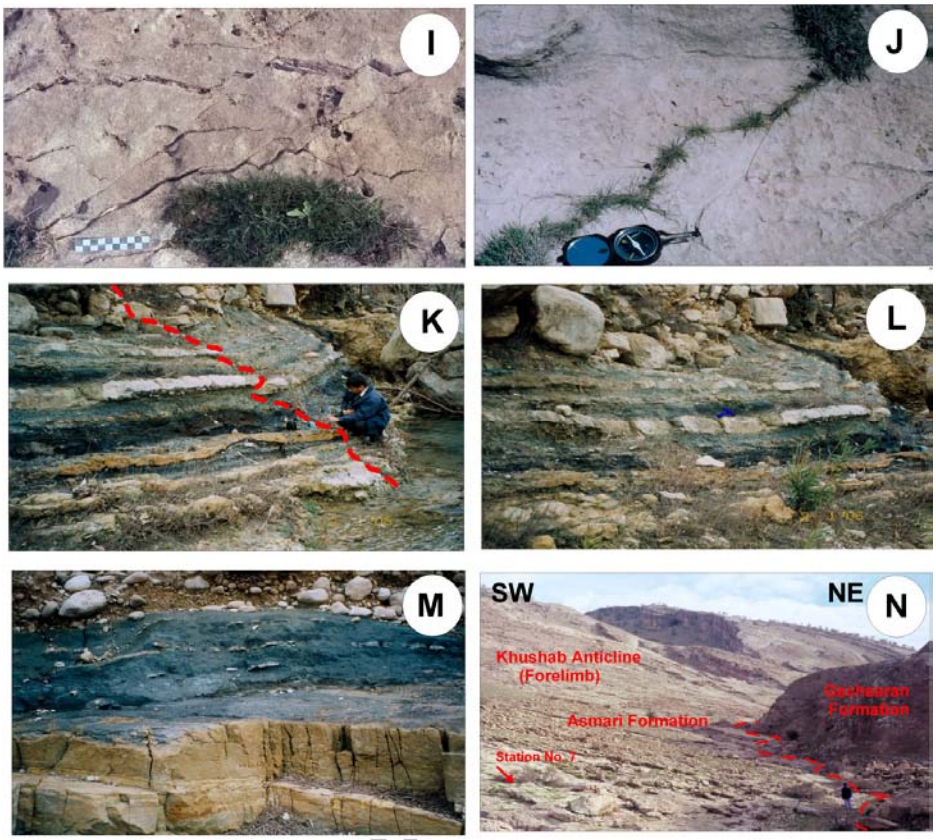

Figure 14. Continued. I, J: Two close up of sigmoidal gash fractures in Asmari Formation in Khushab anticline. Station No. 2. K, L and M: examples of observed boudins in Pabdeh-Gurpi Formation in Khushab anticline. Station No. 5. N: A showing of the contact between Gachsaran and Asmari Formation in forelimb of Khushab anticline. Station No. 7.

the Asmari and Khaviz anticlines and believed that these fractures formed by effect of paleoreleif structures. Also [28] have reported these fractures in the Zagros anticlines. [6] have reported these fractures in Asmari-Jahrum Formations, in Dashtak and Sarbalesh anticlines. The formation of these fractures are attributed to dextral shear zone that affected by the movement of the Kazerun fault zone. Fractures with 075° trending (set D) and fractures with 285° trending (set G) are coincided with trend of R and P shear fractures respectively. Because of R' shear fractures are sampled in a few stations, therefore the less numerous of them is interpreted that neither it is possible they have not been developed, nor the formation of them may be influence by the Balarud fault zone. Therefore due to the treatments of the fault zone prevent the formation of R' shear fractures. The Rit thrust (N60°W) (Fig. 3), which has a sense of shear similar to P shear fractures, is a synthetic fracture as the shear zone. The angle between these shears fractures and the axis of maximum principal stress is 30° [63]. Also, [46] have considered a second-order shear fracture in a shear system. The directions of these oblique fractures which trend 075° and 345°are coincided with the second-order shear fracture with the shear zone in the wrench fault tectonics that is presented by [53]. From these two orientations, only one of them (namely set F with 345° trending) has well developed in present anticline, and another orientation is rare developed. It seems, the development of these fractures is affected by the Balarud fault zone.

The distribution geometry and intensity of fractures in forelimb and backlimb of Khushab anticline indicate that this anticline was formed by fixed-hinge kinematics in the competent unit(s), and was later affected by the Balarud fault zone. Similarity of these fractures systems is confined by [34]'s model, which considers kinematically as variable detachment depth and fixed-

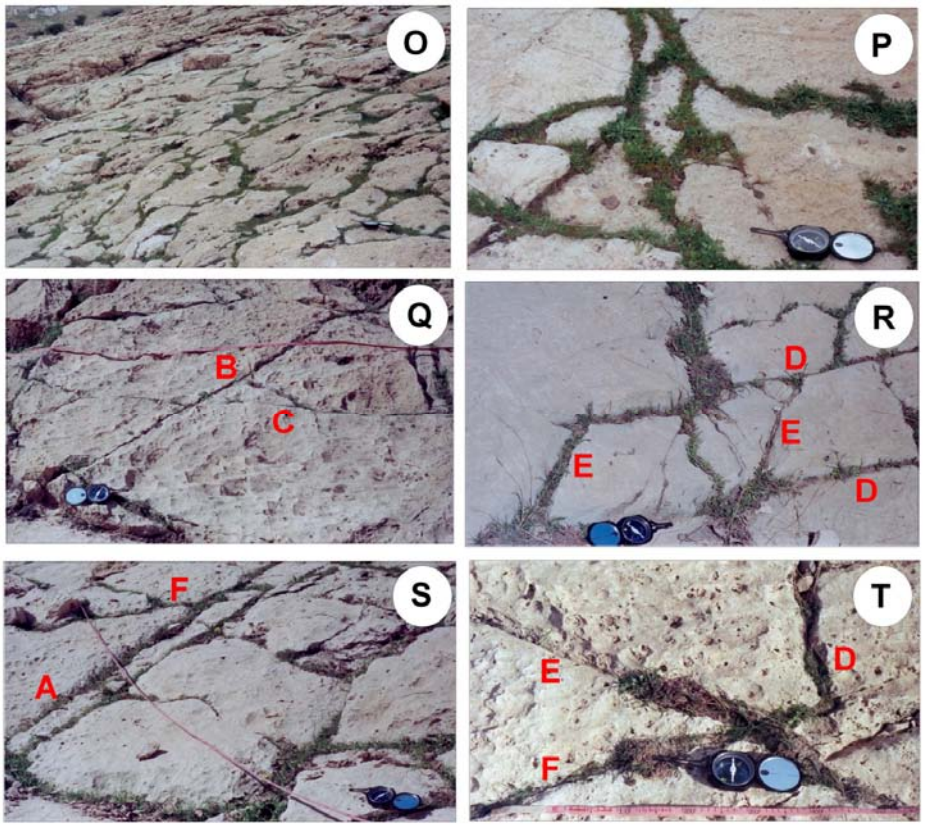

Figure 14. Continued. O, P: A wide (O) and a close up for showing nonsystematic fractures set in Asmari Formation in forelimb of Khushab anticline. Station No. 18. Q: A showing of the relationship between B and C fractures set in Asmari Formation in backlimb of Khushab anticline. Station No. 18. R: An example of D and E fractures set in Asmari Formation in backlimb of Khushab anticline. Station No. 22. S: A showing of A and F fractures set in Asmari Formation in backlimb of Khushab anticline. Station No. 20. T: Relationship between D, E and F fractures set in Asmari Formation in forelimb of Khushab anticline. Station No. 17.

hinge buckle folds in each thin-skinned folded-thrust belts. Also [71] have reported in Kuh-e Pahn and Kuh-e Mish, a basement rooted fault intersects these folds. It will strongly affect both the length and orientation of fractures, due to reactivation. They believed which the north-south and east-west basement trends are best developed and reactivation of secondary shears associated with these trends is common [71].

The ongoing contractional processes involved in the collision between the Iran and the Arabian Plates [10,4,77], which started during the Miocene-Pliocene [10], accounts for folding and faulting of the Zagros Mountains. These processes caused the forming of the orthogonal fractures (A and B sets). The oblique fractures (C, D, E, F, G sets), which are shear fractures in sinistral shear zone, have been created and affected by the Balarud fault zone. These fractures were formed during the late Alpine phases, possibly Plio-Pliostocene (?). Based on previous works [8,9,36], it may be possible to consider two phase for forming of our seven sets fractures that are represented in Fig. 16. A and B sets were formed in first phase (Figs. 16-a, c) and in secondly phase the C, D, E, F and G sets fractures which were oblique with respect to fold axis, were formed (Figs. 16-b, d). The presence of sigmoidal gash fractures in Asmari Formation (Figs. 16-I, J), demonstrated the governing of a deformation with sinistral movement influence by movements of the Balarud fault zone. These fractures which form as the result of shear, correspond well with [64], ([64], Figs. 3, 4-b, page 87). It can be possible formed during the lately Alpian phases, possibly Plio-Pliostocene (?). The effects of the subperpendicular faulted structures in Zagros is now well known and constraint (see [30,85]).

The structure of Khushab anticline in seismic profiles lines 1, 3 and 4 is a simple structure. The upper

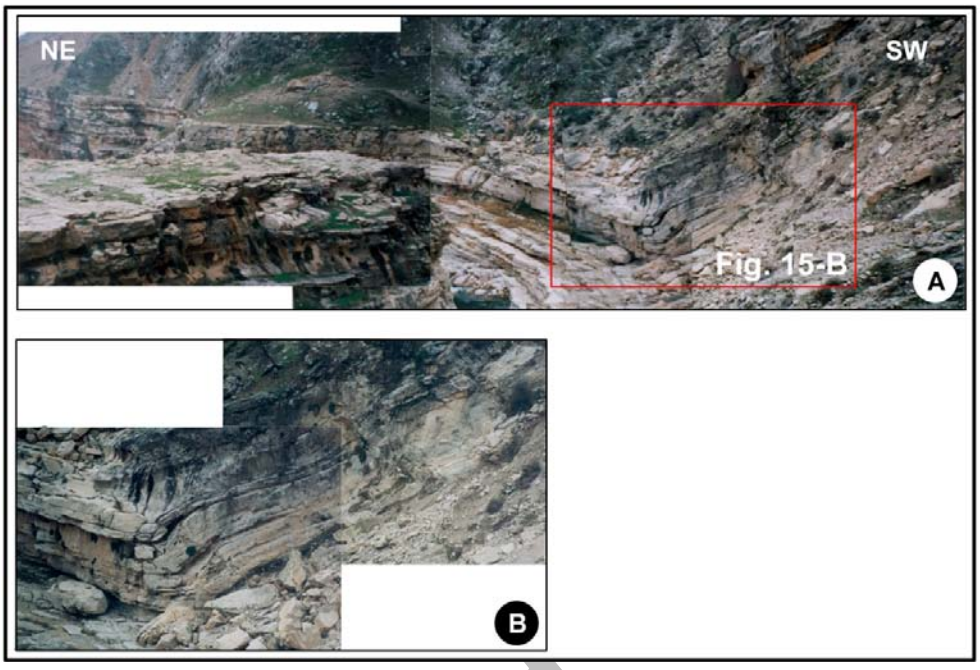

Figure 15. Gerdab syncline in station No. 4 (After [27]). See location on Figure 3.

sedimentary units at the crest remain approximately broad within these seismic profiles (Figs. 5, 7, 8). These seismic profiles are suggested the gently forelimb, in which it has a shallower dip at the crest, and an indistinct backlimb. So it illustrated that the backlimb is very broad and undergoes a slightly bending and the fold geometry at a very early stage of development. The Khushab anticline in HH' cross-section is broader that the FF' cross-section. It can be interpreted that the fault zone do not cut through sedimentary units and these units flattens in two ends of the cross-sections. So this fold does not match the geometry of any fault-bend [73,74,50] or fault-propagation [37,66,76,75] folds models. Previously the folds in the Zagros fold-thrust belt have generally been interpreted as detachment folds above the lower Cambrian Hormoz Salt (e.g. [1,2,16, 44]).The first early researchers (e.g. [72]), and several of lately of them [51,69], have developed the models with characteristic features detachment and faulted detachment folds for this belt. However, the large interlimb angles observed in which anticline (Figs. 10, 11, 13, Table 2) cannot be seen in fault-propagation folding. The anticline may be either a detachment fold with A/h<1 [37], or a transported fault-propagation fold [5,37,42,45]. Interpretation of seismic profiles 3 and 4 (Figs. 7, 8) suggests that the present-day geometry is similar to a detachment fold or a faulted detachment fold.

The Khushab anticline with low amplitude and relatively large wavelength is very similar to Burgerwaldkette anticline [14,40], which is reported as a detachment fold. For all of detachment folds within the Zagros fold-thrust belt, the amplitudes of the folds with respect to the offsets of the faults imply that most folds are affected by faulting [35,67,83]. The backlimb of the Khushab anticline transferred above a bedding-parallel (namely the Balarud fault zone) or on detachment horizon which is possibly Dashtak Formation (?) (Table 1). This transfer is resulted in the growing of the Khushab anticline. During of the growing, the area above a stratigraphically detachment horizon (namely Dashtak Formation ?) should be remain to balance and the amounts of shortening must be simultaneously at all levels within the structure are constant. So displacement goes toward southwest into Chenareh anticline. The Chenareh anticline, which is a fault-propagation fold [26], primarily accommodates by this displacement (Fig. 10). This displacement which is previously calculated [26], produces a deformed footwall in subsurface and a forelimb syncline (namely Gerdab syncline, Fig. 15) at surface. So the kinematic model of Khushab anticline has applicability to thin-skinned fold-thrust belts and possibly indicates that the anticline treats resemble other growing anticlines in the fold-thrust belt. In field the beds (Asmari Formation) of

the forelimb syncline are continuously rotated and are undergone thickness changes. Until they are cut by the propagating fault (Fig. 15).

The Balarud fault zone is not a continually structure in the area between of the Lurestan and Dezful Embayment zones. Interpreted seismic profiles (Figs. 5, 6, 7, 8, 9) do not indicate the fault zone not only a continuously structure but also this structure can be as a segmented fault zone (e.g. in seismic profiles lines 2, 5; Figs. 6, 9). The presence or absence of the Balarud fault zone possibility considers that the fault zone can be as a segmented fault zone on underlying lateral oblique ramps. The measured offset of the Balarud fault zone is about 50 Km based on two seismic profiles lines (Figs. 6, 9) from the crest of anticline.

The stretching of the stiff and thinner carbonate bedding (Gurpi Formation) is achieved by boudinage but the stiff and very much more thickness below these structures is achieved by extensional fractures which are perpendicular to bedding surface. These structures correspond well with previously commonly bodinage structures (e.g. [41]).

In the forelimb of Khushab anticline, a Rabbit Ear structure as a minor anticline, is observed in southwest of the Barikab village (Fig. 3). Formation of this minor structure is related to exciting of the detachment horizons in the younger stratigraphic horizons [69].

The stylolites are observed in Asmari Formation (Figs. 14-G, H), which corresponds with sharp-peak type of classification of stylolites [25]. These structures formed during the shortening time and before end of the folding process and influences of pressure solution [41].

The style of folding in foreland of the many fold-thrust belts becomes subclass 1C to 1B [55], the similarity fold style of study anticline (Table 2), approximately indicates the same subclass.

In the Zagros fold-thrust belt, the reaction of basement to a new stress field will be controlled by the previously existing basement-involved fault zones. The Balarud fault zone, which is one of the active fault zones of these structures, controlled the deformational process in the Lurestan and Dezful Embayment border zones. The Khushab anticline is mainly affected by the Balarud fault zone.

Detailed study of the geometry and kinematics of deformation in Khushab anticline provides the following constraints on the structural evolution of the Balarud fault zone:

(1) The deformation of the sediment sequence of Khushab anticline is largely controlled by, and reflects, activity on the Balarud fault zone, which is a basement-involved [10] and is an oblique lateral ramp [68].

(2) The geometric analysis indicates that this anticline is noncylindrical, asymmetrical and disharmonic fold. The descriptive term of Aspect Ratio for Khushab anticline is from wide to broad. The descriptive term of Bluntness for this anticline is subangular. The class of folding for Khushab anticline is from subclass 1B to 1C.

(3) The geometry of the surface structures (Fractures, Boudins, and Stylolites) was governed by a strong deformation related to thrusting of the Balarud fault zone.

The fracture analyses represented that they are orthogonal (A, B sets) and oblique (C, D, E, F and G sets) fractures with respect to anticline axis. A and B sets fractures which formed in associated with folding, are parallel and perpendicular to fold axis respectively. C, D, E, F and G sets fractures which may be interpreted as shear fractures coincided with the characteristics of fractures in the sinisteral shear zones. It seems two phases are responsible for forming of those fractures systems. A and B sets were formed in first phase and associated with formation of anticline. The other system, C, D, E, F and G fractures sets were formed in second phase and are under effect of the Balarud fault zone.

(4) The occurrence of Khushab anticline, with its specific geometries in the Dashtak Formation (?), which is a detachment horizon, and deformed under the convergence conditions, suggests that this anticline represents early stages in the evolution of detachment folds or faulted detachment folds. Whereas, Chenareh and Barikab [27] anticlines, which are adjacent anticlines in southwest of Khushab anticline, represents

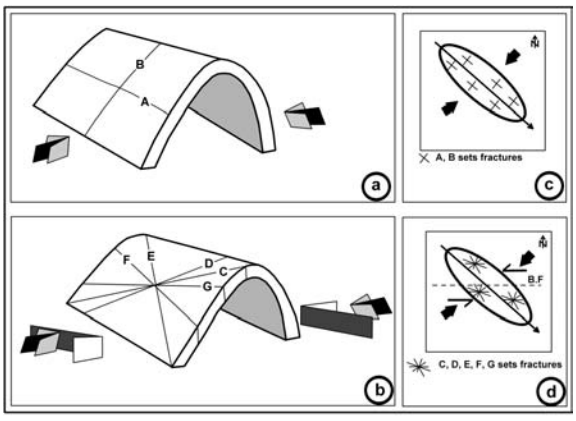

Figure 16. The schematic sketch of two phases that may be considered for forming of seven sets of fractures in Khushab anticline. a, b: block diagram and c, d: map of Khushab anticline. See text for more explanation (B.F = Balarud Fault Zone).

fault-propagation fold.

(5) The changes in the fault geometry, namely the presence or absence of the Balarud fault zone in interpreted seismic profiles, indicate that this fault zone can be as a segmented fault zone on underlying lateral oblique ramps.

Acknowledgements

The authors would like to thank the Management of Exploration director of N.I.O.C for providing part of data used in this study. The authors greatly appreciate the facilities N.I.O.C south oil company during the fieldworks which was several periods in study area. They thank I. Abdollahi Fard for his comments and contribution, which were very helpful in improving the paper.

References

1. Alavi M. Tectonostratigraphic evolution of the Zagrosides of Iran. Geology, 8: 144-149 (1980).
2. Alavi M. Tectonics of Zagros Orogenic Belt of Iran: new data interpretation. Tectonophysics, 229: 211-238 (1994).
3. Alavi M. Regional stratigraphy of the Zagros fold-thrust belt of Iran and its proforeland evolution. American Journal of Science, 304: 1-20 (2004).
4. Allen M., Jackson J. and Walker R. Late Cenozoic reorganization of the Arabia-Eurasia collision and comparison of short-term and long-term deformation rates. Tectonics, 23: PTC2008. (2004).
5. Apotria T. G., Snedden W. T., Spang J. H. and Wiltschko D. V. Kinematics models of deformation at an oblique ramp. In: McClaly, K. R. (Ed.), Thrust Tectonics, London, Chapman & Hall, pp.141-154 (1992).
6. Azizzadeh M. Structural analysis of the Asmari Formation fractures in the Izeh zone its application to hydrocarbon reservoir modeling, Ph.D. *Thesis*, Shahid Beheshti University, 313p. (2007).
7. Baudin T., Marquer D. and Persoz F. Basement-cover relationships in the Tambo nappe (Central Alps, Switzerland): geometry, structure and kinematics. Journal of Structural Geology, 15: 543-553 (1993).
8. Bellahsen N., Fiore P. E. and Pollard D. D. The role of fractures in the structural interpretation of Sheep Mountain Anticline, Wyoming. Journal of Structural Geology, 28: 850-867 (2006).
9. Bellahsen N., Fiore P. E. and Pollard D. D. From spatial variation of fracture patterns to fold kinematics: A geomechanical approach. Geophysical Research Letters, 33: 1-4 (2007).
10. Berberian M. Master blind thrust faults hidden under the Zagros folds: active basement tectonics and surface morphotectonics, Tectonophysics, 241: 193-224 (1995).
11. Berberian M. and Tchalenko J. S. On the tectonics and seismicity of the Zagros active folded belt. Geodynamics of southwest Asia, Tehran symp. Geological survey of Iran (1970).
12. Boyer S. E. and Elliott D. Thrust systems. American Association of Petroleum Geologists Bulletin, 66: 119-123 (1982).
13. Bradley D. C. Description and analysis of early faults based on geometry of fault-bed intersections. Journal of Structural Geology, 11: 1011-1020 (1989).
14. Buxtorf A. Prognosen und Befunde beim Hauensteinbasis und Grenchenberg tunnel und die Bedeutung der letzteren fur die Geologie des Juragebiges. Verhadlungen des Naturforschunden die Gesellschaft Basel, 27: 185-254 (1916).
15. Chester J. S. and Chester F. M. Fault-propagation folds above thrust with constant dip. Journal of Structural Geology, 21: 903-910 (1990).
16. Colman-Sadd S. P. Fold development in Zagros simply folded belt, southwest Iran, American Association Petroleum Geologists Bulletin, 62: 984-1003 (1978).
17. Dahlstrom C. D. A. Structural geology in the eastern margin of Canadian Rocky Mountains, Canadian Petroleum Geology Bulletin, 18: 332-406 (1970).
18. Dahlestrom C. D. A. Geometric constraints derived from the law of conservation of volume and applied to evolutionary models for detachment folding, American Association of Petroleum Geologists Bulletin, 74: 336-344 (1990).
19. Davis G. H. and Reynolds S. J. Structural Geology of Rocks and Regions, John Wiley & Sons, Inc., 776p. (1996).
20. Erickson S. G., Strayer L. M. and Suppe J. Initiation and reactivation of faults during movement over a thrust faults ramp: numerical mechanical models. Journal of Q. J. Geol. Soc. London, 117: 367-376 (2001).
21. Falcon N. L. Southern Iran: Zagros Mountains. In: Spencer, A. (Ed.), Mesozoic-Cenozoic Orogenic Belts. Geological Society of London, Special Publications, 4: 199-211 (1974).
22. Falcon N. L. Problems of the relationship between surface structure and deep displacements illustrated by the Zagros ranges. In: Kent, P. E., Satterthwatte, g. e. and Spencer, A. M. (Eds.), Time and Place in Orogeny. Geological Society, London, pp.9-11 (1969).
23. Geiser P. A. Mechanisms of thrust propagation: some examples and implications for the analysis of overthrust terrenes. Journal of Structural Geology, 10: 829-845 (1988).
24. Glen R. A. Basement control on the deformation of cover basin: an example from the Cobur district in the Lachlan fold belt, Australia, Journal of Structural Geology, 7: 301-315 (1985).
25. Guzzeta G. Kinematics of stylolites formation and physics of pressure solution process. Tectonophysics, 101: 383-394 (1984).
26. Hajialibeigi H., Alavi, S. A., Eftekharnezhad J., Mokhtari M., and Adabi M, H. Geometric analysis of Barikab anticline as a fault-propagation fold affected by the Balarud fault zone, SW Iran, 11th symposium the Geological Society of Iran, Mashhad, (2007).
27. Hajialibeigi H., Alavi, S. A., Eftekharnezhad J., Mokhtari M., and Adabi M, H. Tectonics and deformation pattern of the Balarud fault zone (North of Dezful), Ph.D. Thesis, Shahid Beheshti University, 210 p. (2009).

28. Halsey J. H. and Corrigan A. F. Fracture study. Report of the fracture study team. progress report. National Iranian Oil Company (1977).
29. Hardy S. and Poblett J. Geometric and numerical models of progressive limb rotation in detachment folds. Geology, 22: 371-374 (1994).
30. Hessami K., Koyi H. A., Talbot C., Tabasi, H. and Shabanian E. Progressive unconformities with an evolving foreland fold-thrust belt, Zagros Moutains. Journal of the Geological Society, London, 158: 969-981 (2001).
31. Hodgson R. A. Regional study of jointing in Comb Ridge-Navajo Mountain area, Arizona and Utah: American Association of Petroleum Geologists Bulletin, 45: 1-38 (1961).
32. Hodgson R. A. Reconnaissance of jointing in Bright Angel area, Grand Canyon, Arizona. American Association of Petroleum Geologists Bulletin, 45: 95-97 (1961).
33. Hodgson R. A. Genetic and geometric relations between structures in basement and overlying sedimentary rocks, with examples from Colorado Plateau and Wyoming. American Association of Petroleum Geologists Bulletin, 49: 935-949 (1965).
34. Homza T. X. and Wallace W. K. Geometric and kinematics models for detachment folds with fixed and variable detachment depths. Journal of Structural Geology, 17: 575-588 (1995).
35. Hyett A. J. Deformation around a thrust tip in carboniferous Limestone at Tutt Head, near Swansea, South Wales. Journal of Structural Geology, 12: 47-58 (1990).
36. Ismat Z. Folding kinematics expressed in fracture patterns: an example from the Anti-Atlas fold belt, Morocco, Journal of structural Geology, 30: 1396-1404 (2008).
37. Jamison W. J. Geometric analysis of fold development in over thrust tectonics. Journal of Structural Geology, 9: 207-219 (1987).
38. Jamison W. R. Stress controls on fold thrust style, In: McClaly, K. R. (Ed.), Thrust Tectonics, London, Chapman & Hall, pp.155-164 (1992).
39. James G. S. and Wynd J. G. Stratigraphic nomenclature of Iranian Oil Consortium Agreement Area. American Association of Petroleum Geologists Bulletin, 49: 2182-2245 (1965).
40. Laubscher H. P. Fold development in the Jura. Tectonophysics, 37: 337-362 (1977).
41. Logan B. W. and Semeniuk V. Dynamic metamorphism processes and products in Devonian carbonate rocks. Canning Basin Western Australia. Geological Society of Australia, Special Publication, 6: 11-68 (1976).
42. Lui H., McClay K. R. and Powell D. Physical models of thrust wedges. In: McClaly, K. R. (Ed.), Thrust Tectonics, London, Chapman & Hall, pp.71-81 (1992).
43. MaCleod J. H. and Sahabi F. The Balarud, geological compilation map, Scale1:100 000, Geological and Exploration Division, Tehran, Iranian Oil Operating Companies (1969).
44. McQuarrie N. Crustal scale geometry of the Zagros fold-thrust belt, Iran. Journal of Structural Geology, 26: 519-535 (2004).
45. Mercier E., Quttani F. and De Lamotte D. F. Late-stage evolution of fault-propagation folds: principles and example. Journal of Structural Geology, 19: 185-193 (1997).
46. McKinstry H. E. Shears of the second order, American Journal of Science, 251: 401-414 (1953).
47. McQuillan H. Surface Asmari anticline fracture patterns at airphotograph scale, A comparison with small scale fracture systems. Iranian Oil Operating Companies, Report No. 1134 (1968).
48. McQuillan H. Fracture patterns on Kuh-e-Asmari Anticline, Southwest Iran. American Association Petroleum Geologists Bulletin, 58: 236-245 (1974).
49. Mitra S. and Namson J. S. Equal-area balancing. American Journal of Science. 298: 563-599 (1989).
50. Mitra S. Fault-propagation folds: geometry kinematics evolution and hydrocarbon traps. American Association of Petroleum Geologists Bulletin, 74: 921-945 (1990).
51. Mitra S. Fold accommodations fault. American Association of Petroleum Geologists Bulletin, 86: 671-693 (2002).
52. Mitra S. A unified kinematic model for the evolution of detachment folds. Journal of Structural Geology, 25: 1659-1673 (2003).
53. Moody J. D. Petroleum exploration aspects of Wrench Fault Tectonics, American Association of Petroleum Geologists Bulletin, 57: 449-476 (1973).
54. Motiei H. Geology of Iran: Stratigraphy of Zagros. Geological Survey of Iran 540p. (1995).
55. Moores E. M. and Twiss R. J. Tectonics. W. H. Freedman & Co., New York, 415p. (1995).
56. Mulugeta G. and Koyi H. Three-dimensional geometry and kinematics of experimental piggyback thrusting. Geology, 15: 1052-1056 (1987).
57. Narr W. and Suppe J. Kinematics of basement-involved compressive structures, American Journal of Science, 294: 802-860 (1994).
58. N.I.O.C. Geological map of Iran: south-west Iran, Scale1:1 000 000, National Iranian Oil Company. Exploration and Production, Tehran (1969).
59. O'Brien C. A. E. Tectonic problems of the oilfield belt of southwest Iran, 18th Intern. Geol. Cong. Great Britain, Proc, 6: 45-58 (1950).
60. Poblett J. S. and McClay. K. Geometry and kinematics of single layer detachment folds, American Association of Petroleum Geologists Bulletin, 80: 1085-1109 (1996).
61. Pattinson R. and Takin M. Geological significance of the Dezful Embayment boundaries. Iranian Oil Operation Companies (1971).
62. Pattinson R. and Jazayeri B. Structural analysis of Zagros anticlines. Iranian Oil Operating Companies, Report No. 1188 (1972).
63. Price N. J. and Cosgrove J. W. Analysis of Geological Structural. Cambridge University Press, Cambridge, 502p. (1990).
64. Ramsay J. G. and Huber M. I. The Techniques of Modern Structural Geology, Vol.1: Strain Analysis. Academic Press, London, 307p. (1987).
65. Rich J. L. Mechanics of low angle overthrust faulting as illustrated by Cumberland thrust block, Virginia, American Association of Petroleum Geologists Bulletin, 18:1584-1596 (1934).
66. Ray S. K. Plunging fault-propagation folds: a case study

from the Bhutan Himalayas. In: Sengupta, S. (Ed.), Evolution of geological structures in micro-to macro-scales. London, Chapman & Hall, pp.91-110 (1997).
67. Sattarzadeh Y., Cosgrove J. W., and Vita-Finzi C. The interplay of faulting and folding the evolution of the Zagros deformation Belt. In: Cosgrove, J. W. and Ameen, M. S. (Eds.) Forced folds and Fractures. Geological Society of London, 169: 187-196 (2000).
68. Sepehr M. and Cosgrove J. W. Structural framework of the Zagros fold-thrust belt, Iran. Marine and Petroleum Geology, 21: 829-843 (2004).
69. Sherkati S., Molinaro M. de Lamotte D. F. and Letouzay J. Detachment folding in the central and eastern Zagros fold-belt (Iran): salt mobility, multiple detachments and the final basement control. Journal of Structural Geology, 27: 1680-1696 (2005).
70. Silliphant L. J., Englder T. and Gross M. R. The state of stress in the limb of the Split Mountain Anticline, Utah: Constraints placed by transected joints. Journal of Structural Geology, 24: 155-172 (2002).
71. Stephenson B. J., Koopman A., Hillgartner H., McQuillan H., Bourne S., and Rawnsley K. Structural and stratigraphic controls on fold-related fracturing in the Zagros Mountain Iran: implications for reservoir development. In: Lonergan, L., Jolly, R. J. H., Rawnsley, K. and Sanderson, D. J. (Eds). Fractured Reservoirs, Geological Society, London, Special Publication, 270: 1-21 (2007).
72. Stocklin J. Structural history and tectonics of Iran: a review. The American Association of Petroleum Geologists Bulletin, 52: 1229-1258 (1968).
73. Suppe J. Principles of structural geology, Prentice Hall, Englewood Cliff, New Jersey, 537p. (1985).
74. Suppe J. Chou G. T. and Hook S. C. Rates of folding and faulting determined from growth strata. In: McClaly, K. R. (Ed.), Thrust Tectonics, London, Chapman & Hall, pp. 105-121 (1992).
75. Suppe J. and Medwedeff D. A. Fault-propagation folding. Geological Society of America Abstracts with Programs, 16: 670 (1984).
76. Suppe J. and Medwedeff D. A. Geometry and kinematics of fault propagation folding. Eclogae Geologicae Helvetiae, 83: 409-453 (1990).
77. Tatar M., Hatzfeld D. and Ghafory-Ashtiany M. Tectonics of the Central Zagros (Iran) deduced from microearthquake seismicity. Geophy J. Int., 156: 255-266 (2004).
78. Tchalenko J. S. The evolution of kink bands and the development of compression textures in sheared clays, Tectonophysics, 6: 159-174 (1986).
79. Thomas W. A. Continental margins, orogenic belts and intracratonic structures, Geology, 11: 270-272 (1983).
80. Throbjornsen K. L. and Dunne W. M. Origin of a thrust-related fold: Geometric vs. kinematics tests. Journal of Structural Geology, 19: 303-319 (1997).
81. Twiss R. J. and Moores E. M. Structural Geology. W. H. Freedman & Co., New York, 532p. (1992).
82. Twerenbold E. F., Raualx S. J. and Van Os B. Fracture pattern study of Kuh-e-Bangestan and its bearing on oil accumulation. National Iranian Oil Company (1962)
83. Wallace W. K. and Homza T. X. Detachment folds versus fault-propagation folds and their truncation by thrust faults. In: McClaly, K. R. (Ed.), Thrust Tectonics and hydrocarbon systems. American Association of Petroleum Geologists Bulletin, memoir, 82: 324-355 (2004).
84. Wise D. U. Microjointing in basement, middle Rocky Mountain of Montana and Wyoming, Geological Society of America Bulletin, 75: 287-306 (1964).
85. Yassaghi A. Integration of Landsat imagery interpretation and geomagnetic data on verification of deep-seated transverse fault lineaments in SE Zagros, International. Journal of Remote Sensing, 27: 4529-4544 (2006).